International Communications in Heat and Mass Transfer 70 (2016) 127–131

Contents lists available at ScienceDirect

International Communications in Heat and Mass Transfer

journal homepage: www.elsevier.com/locate/ichmt

Effect of non-condensable gas on laminar film condensation of steam in horizontal minichannels with different cross-sectional shapes☆

Zhan Yin, Jianjun Wen, Yining Wu, Qiuwang Wang, Min Zeng *

Key Laboratory of Thermo-Fluid Science and Engineering, Ministry of Education, Xi'an Jiaotong University, Xi'an, Shaanxi 710049, China

ARTICLE INFO

Available online 21 November 2015

Keywords:
Condensation
Non-condensable gas
Minichannel
Cross-sectional shape

ABSTRACT

In the present study, a 3-D numerical simulation of laminar film condensation of steam in the presence of non-condensable gas is performed in horizontal minichannels with six cross-sectional shapes based on the volume of fluid (VOF) method. Mixture of steam and oxygen enters the channel with uniform temperature, while the inlet volume fraction of oxygen increases from 0% to 3%. It is shown that the existence of non-condensable gas results in significant reduction in the mass transfer rate from vapor to liquid along the interface in the axial direction. And then the heat transfer coefficient of condensation with oxygen is demonstrated to decline sharply compared with that of the pure vapor condensation.

1. Introduction

During vapor condensation in the industrial applications, such as turbine plant, condenser in air conditioner, and electronic devices, condensation plays an important role because of its excellent heat transfer performance. However, vapor always mixes with some species that may not condense depending on different working conditions [1], and the non-condensable gas will have a negative effect on condensation heat transfer. For example, less than 1% (by mass) of air in steam condensation can make the condensation heat transfer coefficient drop by more than half, induced by a concentration of non-condensable gas near the vapor–liquid interface [2]. Therefore, condensation in the presence of non-condensable gas has attracted great attention in the recent years.

Minkowycz and Sparrow [3] developed an analytical investigation of laminar film condensation of steam on a vertical isothermal plate in the presence of air. The results indicated that the influence of the non-condensable gas on the heat transfer was accentuated at lower pressure levels, and the effect of superheating on condensation in the presence of a non-condensable gas was much more significant than that in the case of pure vapor condensation. In the recent years, numerical simulation of condensation with non-condensable gas mainly depended on the solution of the boundary layer equations [4–8]. The double boundary layer model was developed by Tang et al. [4] to study the film condensation with air outside a horizontal tube. By solving the coupled heat and mass transfer simultaneously with the finite difference method, the performance of condensation heat transfer was found to deteriorate dramatically even with a little air, which agreed well with the experimental data.

Some experiments have also been performed to investigate the condensation heat transfer in the presence of non-condensable gas. The effect of air on condensation heat transfer in horizontal tubes was investigated experimentally by Ren et al. [9]. The results showed that the overall heat transfer coefficient decreased with higher inlet non-condensable gas mass fraction and higher inlet pressure. In addition, two correlations were developed for the stratified flow and annular flow regimes, respectively. An experiment at atmospheric pressure varying the air concentration was conducted by Chung et al. [10] to analyze the condensation heat transfer of steam–air mixture on a vertical flat plate. It was found that the mixture flow would enhance the heat transfer substantially.

The studies above indicate that the laws of condensation have not been totally clarified yet. In addition, the influence of non-condensable gas in non-circular minichannels has hardly been discussed before. Therefore, a numerical simulation of steam condensation with non-condensable gas in horizontal minichannels with different cross-sectional shapes is conducted by the VOF method in ANSYS FLUENT [11].

2. Numerical model

2.1. Physical model

Totally, six three-dimensional horizontal minichannels with different cross-sectional shapes are adopted. The hydraulic diameter and length of the channels are 1 mm and 50 mm, respectively. The detailed cross-sectional shapes include circular, square, rectangular (aspect ratio of 2 in two directions), and equilateral triangular (regular and inverted),

☆ Communicated by W.J. Minkowycz.
* Corresponding author.
E-mail address: zengmin@mail.xjtu.edu.cn (M. Zeng).

http://dx.doi.org/10.1016/j.icheatmasstransfer.2015.11.008
0735-1933/

Nomenclature

c_p	Specific heat, J/(kg · K)
$\vec{F}$	Surface tension, N/m^3
$\vec{g}$	Gravity, m/s^2
h	Heat transfer coefficient, W/(m^2 · K)
k	Thermal conductivity, W/(m·K)
L_H	Latent heat of vapor, J/kg
$\dot{m}$	Mass source due to phase change, kg/(m^3·s)
n	Categories of phases
p	Pressure, Pa
r	Mass transfer coefficient, s^{-1}
T	Temperature, K
$\vec{v}$	Velocity, m/s
W	Mass fraction of non-condensable gas, %

Greek symbols

α	Volume fraction, %
μ	Dynamic viscosity coefficient, Pa·s
ρ	Density, kg/m^3
φ	Physical property

Subscripts

g	Non-condensable gas
l	Liquid phase
oxy	Oxygen
s	Saturation

Abbreviation

VOF	Volume of fluid

as shown in Fig. 1. The temperature of the mixture at the inlet is the saturation temperature of the vapor at atmospheric pressure. The inlet volume fraction of the non-condensable gas varies from 0% to 3%, while the inlet velocity of the mixture and the wall temperature of the tube wall remain constant at 10 m/s and 353.15 K, respectively.

2.2. VOF method

VOF method is a widely used approach for the numerical simulation of multiphase flow, which belongs to the Euler–Euler multiphase models [11]. It is a surface-tracking technique that can model two or more immiscible fluids by solving a single set of momentum equations and tracking the volume fraction of each of the fluids throughout the domain.

In the VOF method, a phase will be designated as the primary phase, and the other phases are the secondary phases. The volume fractions of the secondary phases are obtained by solving the volume fraction equation of the corresponding phase, while that of the primary phase is achieved based on the theory that the volume fractions of all phases equal to unity. In the present study, the vapor is defined as the primary phase. Therefore, the volume fraction equations of the liquid; non-condensable gas and mixture are presented in the following way:

$$\nabla \cdot \left(\alpha_l \rho_l \vec{v}\right) = \dot{m} \tag{1}$$

$$\nabla \cdot \left(\alpha_g \rho_g \vec{v}\right) = 0 \tag{2}$$

$$\nabla \cdot \left(\rho \vec{v}\right) = 0 \tag{3}$$

In the above equations, subscripts l and g represent the liquid and non-condensable gas, respectively. In Eq. (1), $\dot{m}$ is the mass source due to the phase change from vapor to liquid. However, there is no mass transfer between the gas and other phases in the condensation process with non-condensable gas. As a result, the mass source in Eq. (2) is 0. The velocity in the equations above is shared among all the phases, as well as for the temperature distribution. Hence, the momentum equation and energy equation are as follows:

$$\nabla \cdot \left(\rho \vec{v} \vec{v}\right) = -\nabla p + \nabla \cdot \left[\mu\left(\nabla \vec{v} + \nabla \vec{v}^{T}\right)\right] + \rho \vec{g} + \vec{F} \tag{4}$$

$$\nabla \cdot \left(\vec{v}\left(\rho c_p T + p\right)\right) = \nabla \cdot (k \nabla T) + L_H \dot{m} \tag{5}$$

where $\vec{F}$ and L_H represent the surface tension and the latent heat of vapor, respectively. The physical properties of the multiphase flow shown in the equations above will be assigned based on the local volume fraction and physical properties of each phase:

$$\varphi = \sum_{1}^{n} \alpha_q \varphi_q \text{ with } \varphi = \rho, k, \mu \tag{6}$$

$$\varphi = \frac{1}{\rho} \sum_{1}^{n} \alpha_q \rho_q \varphi_q \text{ with } \varphi = c_p \tag{7}$$

where n represents the categories of phases.

In the present study, a steady state simulation with implicit formulation is performed. The pressure–velocity coupling is handled by means of the SIMPLEC algorithm, while the PRESTO! scheme is adopted for the pressure interpolation. The QUICK scheme is employed for the momentum, VOF, and energy equations.

2.3. Phase change model

As the standard VOF method is applied for the multiphase flow without phase change, a phase change model is needed during the application of the VOF method for the numerical simulation of condensation.

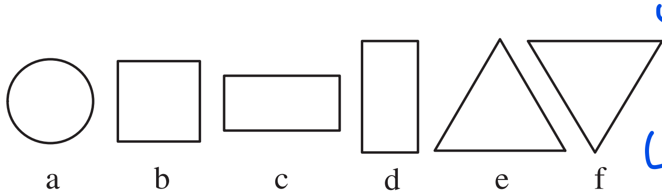

Fig. 1. Schematic of the minichannels with different cross-sectional shapes: (a) circular, (b) square, (c) horizontal rectangular, (d) vertical rectangular, (e) regular equilateral triangular, (f) inverted equilateral triangular.

ضریب انتقال حرارت بخار خالص

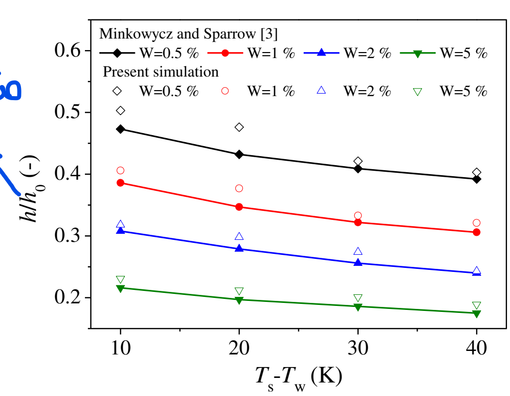

Fig. 2. Validation of the numerical model.

The phase change model adopted in the present simulation is shown as follows:

$$\dot{m} = -r\alpha_l\rho_l(T - T_s)/T_s,\ T \geq T_s \tag{8}$$

$$\dot{m} = r\alpha_v\rho_v(T_s - T)/T_s,\ T \leq T_s \tag{9}$$

The two equations above express the mass transfer between the vapor phase and the liquid phase shown in Eq. (1). The evaluation of r is completed by a previous study on steam condensation in horizontal circular minichannel [12], and $r = 50000\ \mathrm{s}^{-1}$ is chosen in the present study. In addition, the gas-induced saturation temperature difference of the vapor during the condensation with non-condensable gas is less

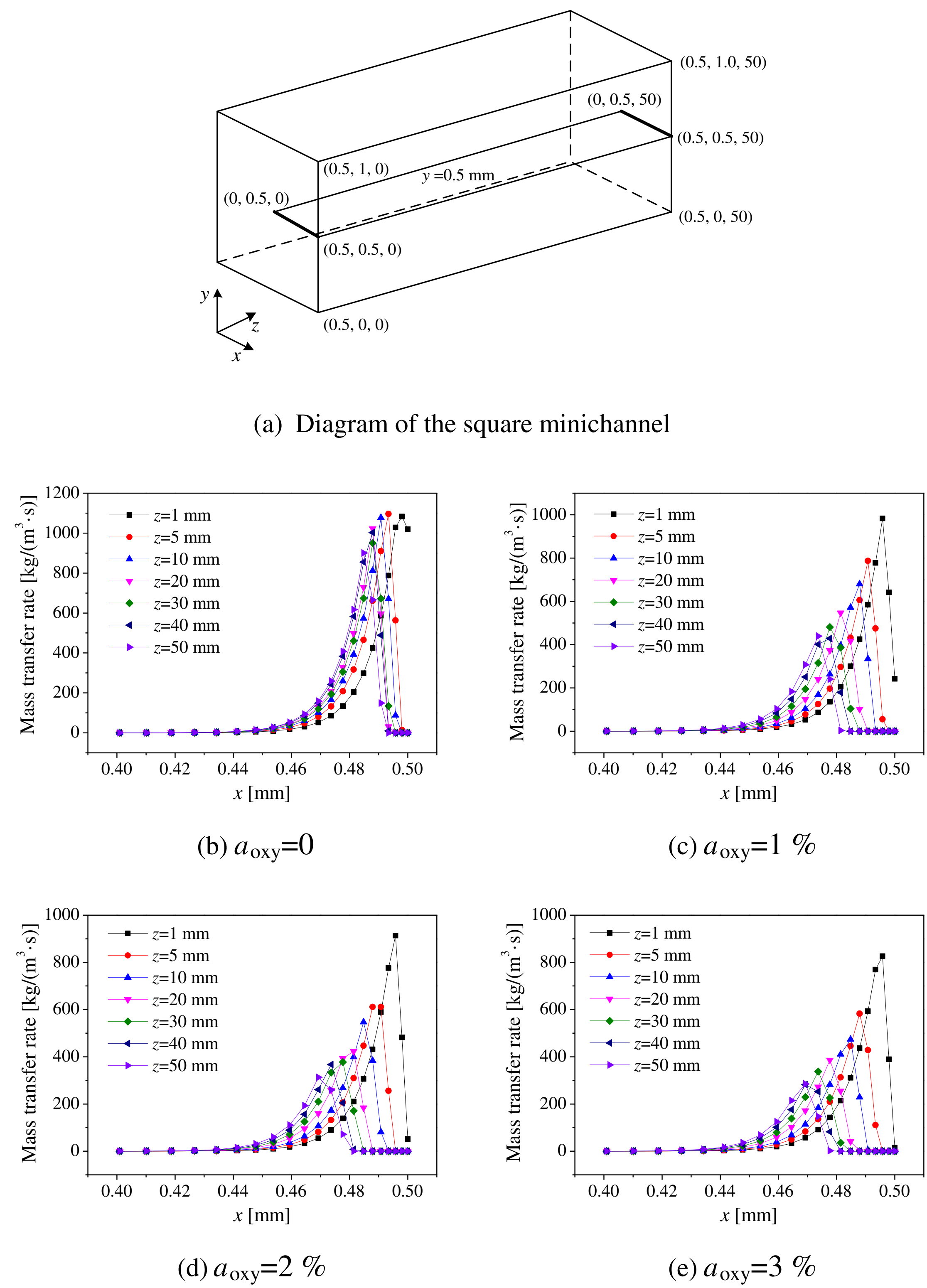

Fig. 3. Mass transfer rate along the axial direction with different inlet volume fraction of oxygen in the square minichannel.

than 1 K because of the relatively small inlet volume fraction of the non-condensable gas and therefore neglected in the present simulation. As a result, the same coefficient is also applied for the numerical simulation of condensation with non-condensable gas.

3. Results and discussions

3.1. Validation of the numerical model

Firstly, as studies on condensation inside horizontal minichannels in the presence of non-condensable gas are scarce, a numerical simulation of laminar film condensation of steam with air on a vertical plate is performed, in order to validate the present numerical model. The comparison between the present result and the analytical investigation of Minkowycz and Sparrow [3] is shown in Fig. 2. The aspect of heat transfer coefficient of condensation with non-condensable gas and that of pure vapor condensation is depicted versus different temperature differences between saturation temperature and wall temperature. The average over-prediction is about 5.8%, which illuminates that the present simulation method of condensation with non-condensable gas is convincing.

Then, a mesh independence test is carried out in the numerical simulation of the condensation in the circular minichannel. The mesh is

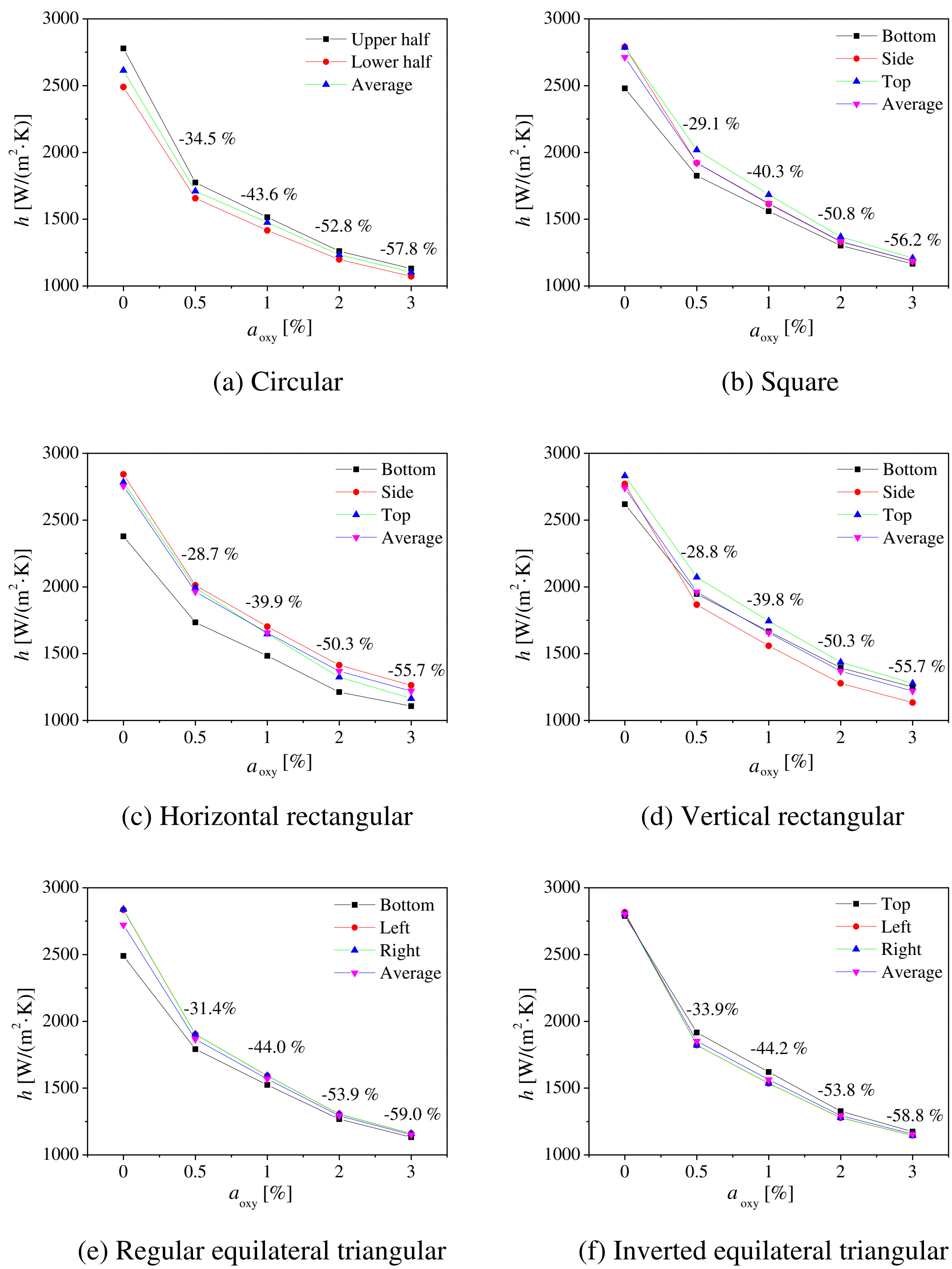

Fig. 4. Condensation heat transfer coefficient of the minichannels.

finer near the wall compared with that in the other place. Totally, 7 sets of meshes displaying 0.18–2.4 M hexahedral cells have been tested, and the difference between the total heat fluxes on the tube wall of the last two meshes is 1.14%. Finally, the mesh with 1.5 M hexahedral cells is chosen, and the similar settings are applied for the mesh generation in the minichannels with non-circular cross-sectional shapes. The mesh sizes differ from 1.5 M to 3.9 M in different channels caused by the difference in the cross-sectional area under the same hydraulic diameter.

3.2. Effect of non-condensable gas on the heat transfer characteristic

In the present study, oxygen is selected as the non-condensable gas. It is well known that a gas layer will exist during the condensation process with non-condensable gas, and the gas layer is proved to augment the resistance during the mass transfer rate from vapor to liquid. Take the condensation process in the square channel as example, the schematic of which is depicted in Fig. 3(a), the mass transfer rates near the wall along the x direction on the cross-section $y = 0.5$ mm at different longitudinal cross-sections are shown in Fig. 3(b–e). For the pure vapor condensation displayed in Fig. 3(b), it can be found that because there is only one phase in the near wall region and the central region of the channel, the mass transfer rates from vapor to liquid equal to 0. Between the two regions above, high mass transfer rates exist near the vapor–liquid interface. And the peak of the curves along the axial direction is moved far away from the wall because of the thicker liquid film induced by the condensation process. The maximum value remains relatively high and is just reduced from 1100 $kg \cdot m^{-3} \cdot s^{-1}$ to 900 $kg \cdot m^{-3} \cdot s^{-1}$. However, it is quite different for the condensation process in the presence of oxygen, as demonstrated in Fig. 3(c–e). The maximum value is declined markedly along the axial direction, when the inlet volume fraction of the oxygen increases from 1% to 3%. And the peak values of all curves in any figure are shifted to the central region much more obviously as a result of the existence of the oxygen layer.

From the analysis above, it can be concluded that the condensation process is severely blocked by the non-condensable gas. In consequence, the average heat transfer coefficients of condensation with oxygen descend sharply, as exhibited in Fig. 4. For all minichannels, a little oxygen with an inlet volume fraction of 0.5% leads to a significant reduction of 30.4 % on an average. However, the declining trend of the average heat transfer coefficient slows down as the inlet volume fraction of the oxygen continues to grow. The maximum inlet volume fraction gives rise to a maximum decrease of 57.1%. It can also be discovered that for the pure vapor condensation in minichannels other than the inverted triangular shape, the heat transfer coefficient on the bottom surfaces is obviously lower than that on the other surfaces, which results from the water liquid accumulation on the bottom surface during pure vapor condensation. The existence of oxygen leads to less condensate liquid, and the difference of heat transfer coefficient on different surfaces is less significant.

4. Conclusions

This paper presents a 3-D numerical simulation of steam condensation with non-condensable gas in minichannels with different cross-sectional shapes. The study is based on the VOF method in ANSYS FLUENT accompanied with a phase change model interpreted by a user-defined function. The oxygen is designated as the non-condensable gas, while the flow in all phases is laminar and incompressible. After saturated vapor with oxygen enters the minichannels with uniform velocity, condensation occurs under the temperature difference between the constant wall temperature and the interface temperature, which is assumed to be equal to the saturation temperature of the steam at atmosphere pressure. The inlet volume fraction of oxygen increases from 0% to 3%. The following conclusions can be drawn:

(1) Under the effect of the oxygen layer existing between the vapor phase and the liquid phase, the mass transfer rate from vapor to liquid along the interface is significantly reduced.
(2) The heat transfer coefficient of condensation with non-condensable gas descends sharply compared with that of the pure vapor condensation.
(3) The difference of heat transfer coefficient on different surfaces of minichannels other than the inverted triangular shape is less significant in condensation with oxygen than that in the pure vapor condensation.

Acknowledgement

This present study is supported by the National Natural Science Foundation of China (grant no.51276139).

References

[1] S.G. Kandlikar, Handbook of phase change: boiling and condensation, CRC Press, 1999.
[2] J.G. Collier, J.R. Thome, Convective boiling and condensation, Oxford University Press, 1994.
[3] W.J. Minkowycz, E.M. Sparrow, Condensation heat transfer in the presence of non-condensables, interfacial resistance, superheating, variable properties, and diffusion, Int. J. Heat Mass Transf. 9 (10) (1966) 1125–1144.
[4] G.H. Tang, H.W. Hu, Z.N. Zhuang, W.Q. Tao, Film condensation heat transfer on a horizontal tube in presence of a noncondensable gas, Appl. Therm. Eng. 36 (2012) 414–425.
[5] V.D. Rao, V.M. Krishna, P.K. Sarma, K.V. Sharma, Convective condensation of vapor in laminar flow in a vertical parallel plate channel in the presence of a high-concentration noncondensable gas, J. Heat Transf. 131 (1) (2009) 011502.
[6] C.O.K. Chen, Y.T. Lin, Turbulent film condensation in the presence of non-condensable gases over a horizontal tube, Int. J. Therm. Sci. 48 (9) (2009) 1777–1785.
[7] C.O.K. Chen, Y.T. Lin, Laminar film condensation from a downward-flowing steam-air mixture onto a horizontal circular tube, Appl. Math. Model. 33 (4) (2009) 1944–1956.
[8] D.Y. Shang, L.C. Zhong, Extensive study on laminar free film condensation from vapor–gas mixture, Int. J. Heat Mass Transf. 51 (17-18) (2008) 4300–4314.
[9] B. Ren, L. Zhang, H. Xu, J. Cao, Z. Tao, Experimental study on condensation of steam/air mixture in a horizontal tube, Exp. Thermal Fluid Sci. 58 (2014) 145–155.
[10] B.J. Chung, S. Kim, M. Chan Kim, An experimental investigation of film condensation of flowing mixtures of steam and air on a vertical flat plate, Int. Commun. Heat Mass Transfer 31 (5) (2004) 703–710.
[11] Ansys Fluent 12.0 Theory Guide, ANSYS Inc, USA, 2009.
[12] Z. Yin, Y. Guo, B. Sunden, Q. Wang, M. Zeng, Numerical simulation of laminar film condensation in a horizontal minitube with and without non-condensable gas by the VOF method, Numer. Heat Transfer, Part A Appl. 68 (9) (2015) 958–977.